Torque Ripple Reduction and Speed Performance of BLDCM Drive with Hysteresis Current Controller

Bikram Das
Assistant Professor, Department of Electrical Engineering
National Institute of Technology, Agartala
Tripura, India

Mahua Chanda
PG Scholar, Department of Electrical Engineering
National Institute of Technology, Agartala
Tripura, India

***Abstract*— This paper illustrates modeling, simulation and comparative analysis of a closed-loop control system with and without Hysteresis Current Controller for Brushless DC motor (BLDCM) drive system. Brushless DC motors can offer great advantage compared to other machines used in industrial and automotive applications due to high torque density, compactness, simpler controller and lower maintenance. BLDC motor is faster, highly efficient, noiseless operation and reliable. BLDC motor control is generally required to measure the speed and position of rotor by using the sensor because the inverter phases must be commutated depending on the rotor position. The BLDC motor, PID speed controller, Hysteresis Current Controller, inverter and commutation logic block has been modeled using different modules and simulated in MATLAB Simulink. Proportional-Integral-Derivative (PID) tuning algorithm is used to control the speed of the motor. An improved model with Hysteresis Current Controller is implemented with the speed feedback loop to provide naturally current protection and torque dynamic control. Some simulation results and comparative waveforms were carried out using MATLAB Simulink version 7.10.0.499 (R2010a) to verify the proper modeling as well as functionality of the controller.**

***Keywords*— *BLDC motor drive, Hysteresis Current Controller, inverter switching, PID, Simulink*.**

I. INTRODUCTION

Brushless DC motor modeling, controlling and performance analysis has become an important aspect of research work in recent days. The use of environment friendly electronics is being developed to save the energy consumption of various devices. This leads to the development in brushless DC motor. It is rapidly becoming the natural choice for applications demanding high reliability and high efficiency. These motors need to operate more efficiently which can significantly affect the performance of many critical applications in the industries, especially in the areas of appliances production, medicine, aeronautics, medical equipment, chemical, automotive, textile, industrial automation as the energy and cost savings becomes a bigger concern for designers of electronic devices [1].

For power distribution to BLDC motors, it uses electrical commutation instead of mechanical. Mounted three hall sensors in the motor are used to determine the rotor's position, which is passed to the electronic controller ensures spinning of the motor at right time and right orientation [2]. The main component of Hall Effect sensors is the magnetic field of either permanent magnet or electromagnet. These magnetic sensors provide the accurate correcting current to the motor coils to make the magnets rotate at the right orientation.

Despite the tremendous advantages of BLDC motors, they possess a limiting factor. To mention, BLDC motor exhibits torque pulsations. These pulsations can cause acoustical noises and vibration which can reduce the performance in highly precised stable applications. In high speed applications, torque pulsations can be filtered out by the inertia of the load. But at low speeds, torque pulsations are most noticeable and can greatly limit motor performance. However to minimize commutation torque ripple various methods are being used in motor drive control strategies [3][4]. Hysteresis Current Controller is one of the simple PWM current control technique and easiest way to implement.

Finally, the aim of the paper is to simulate a closed-loop speed control system by using PID controller and a Hysteresis Current Controller loop is added with the speed feedback loop and hence to observe the improvement in the system performance with low torque ripples. And also, to analyze the different parameters of the motor like speed, torque, phase currents, hall sensors output etc.

II. MOTOR THEORY AND OPERATION

A brushless DC motor is a synchronous motor powered by DC power and is electronically commutated. It employs a dc power supply switched to the three phase stator windings of the motor by semiconductor power devices of the inverter. Rotor position of the motor determines the switching sequence. Like all other motors, BLDC motors also have a rotor and a stator.

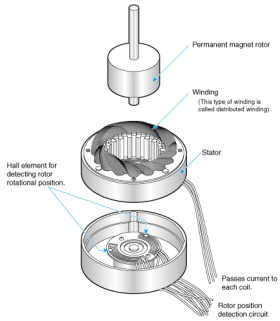

Fig. 1: Disassembled view of BLDC motor

The disassembled view of BLDC motor is shown in the Fig. 1. The primary difference between brushed DC and BLDC motors lies in the type of commutation. Commutation is the act of changing the three phase currents of the motor at appropriate times to produce rotational torque. Brushed DC motors use brushes to commutate the motor. In BLDC motor, the commutator of the brush DC motor is replaced by electronic switches which supply current to the motor windings as a function of the rotor position. The performance of BLDC motor is almost similar to the traditional DC motor with commutator [5].

BLDC motor has many advantages over brushed DC motors and induction motors like high dynamic response, better speed versus torque characteristics, high efficiency, long operating life, noiseless operation and highly reliable. Fig. 2 shows that the torque remains constant for a speed range up to the rated speed in BLDC motor. The motor can be loaded upto the rated torque during continuous operations, but it can be run upto the maximum speed, which is upto 150% of the rated speed. During that time, the torque starts dropping [6].

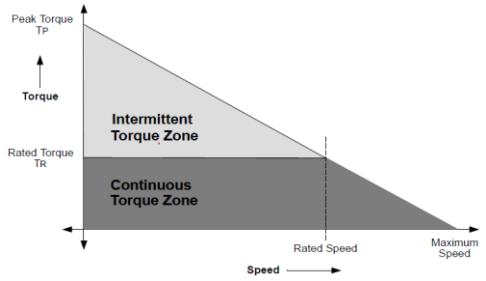

Fig. 2: Torque v/s speed characteristics loop

III. Inverter Switching and Commutation Sequence

For a three phase BLDCM application, the most commonly used topology is a three phase voltage source inverter. The conventional inverter drive system for a BLDC motor is shown in Fig. 3. The three phase inverter operation can be divided into six modes (1-6) according to the current conduction states and conduction sequence. The switches are operated in such a way that each phase conducts only during the 120^0 period when the back emf is constant. Thus, there is a commutation event between phases for every 60^0 electrical, as shown in Fig. 4.

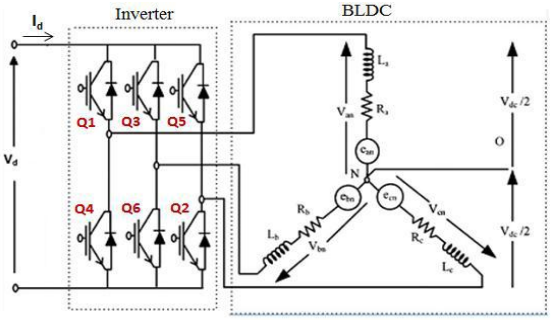

Fig. 3: Conventional BLDC motor drive system

An appropriate commutation therefore requires the knowledge of rotor position, which can be directly detected using hall sensors. The trapezoidal commutation method is the simplest and easiest way to implement the control aspects of BLDC motor. Each hall sensor is typically placed 120^0 apart and produces "1" whenever it faces the North Pole of the rotor [7]. Table-1 shows the motor rotation sequence in clockwise direction. The three phase currents are controlled to take a form of quasi square waveform in order to synchronize with the trapezoidal back emf to produce constant torque.

TABLE I. Sequence for Motor Rotation

Hall Sensors Input States			Active Inverter Switches		Phase Current		
H2	H1	H0	H	L	A	B	C
1	0	1	Q1	Q6	+	−	off
1	0	0	Q1	Q2	+	off	−
1	1	0	Q3	Q2	off	+	−
0	1	0	Q3	Q4	−	+	off
0	1	1	Q5	Q4	−	off	+
0	0	1	Q5	Q6	off	−	+

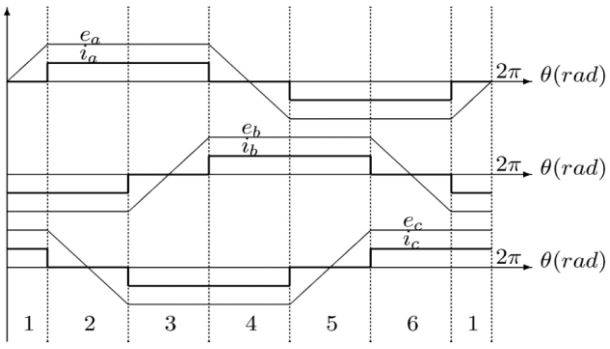

Fig. 4: Back emf and phase current waveform

IV. Mathematical Modeling of BLDC Motor

The modeling of star-connected, three phase brushless dc motor with n-pole permanent magnet rotor involves solving many simultaneous differential equations, each depending upon the inputs to the motor and the motor parameters. The model equations of a BLDC motor are composed of a voltage

equation, a torque equation and a motion equation. Motor parameters are like the phase inductance, phase resistance.

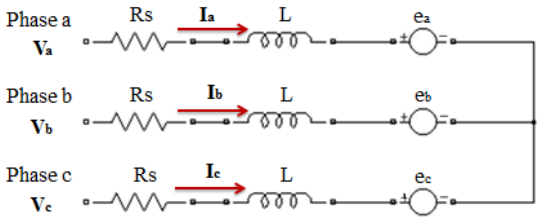

Fig. 5: Equivalent circuit diagram

BLDC motor model is composed of two parts 1) Electrical part which calculates electromagnetic torque and current of the motor. 2) Mechanical part which generates revolution and speed of the motor. The analysis is based on the following assumptions for simplification (i) The motor is not saturated (ii) Stator resistances (suppose, $R_s = R_a = R_b = R_c$) of all the windings are equal and self & mutual inductances are constant (iii) Power semiconductor devices in the inverter are ideal (iv) Iron losses are negligible[8].

A. Voltage Equation:

Applying Kirchhoff's voltage law in the equivalent circuit diagram of BLDC motor as shown in Fig. 5, the coupled circuit equations of the stator windings in terms of motor electrical constants [9] are,

$V_a = I_aR_s + L\,(dI_a/dt) + e_a$
(1)
$V_b = I_bR_s + L\,(dI_b/dt) + e_b$
(2)
$V_c = I_cR_s + L\,(dI_c/dt) + e_c$
(3)

where, V_a, V_b and V_c are the phase voltages and I_a, I_b and I_c are the phase currents. R_s, L are the stator phase resistance and self-inductance respectively. e_a, e_b and e_c are the back emf of phase a, b and c.

The back emf voltages are functions of the rotor mechanical speed ω_m and the rotor angle θ, that is

$e_a = K_e.f(\theta).\omega_m$
(4)
$e_b = K_e.f(\theta - 2\pi/3).\omega_m$
(5)
$e_c = K_e.f(\theta - 2\pi/3).\omega_m$
(6)

The coefficients K_e is the back emf constant. In this model, an ideal trapezoidal waveform profile is assumed.

B. Torque Equation:

The generated electromagnetic torque is given by:
$T_e = (e_a I_a + e_b I_b + e_c I_c)/\omega_m$
(7)

The torque equation for 3-phase are as follows:

$T_a = K_t.I_a.f(\theta)$
(8)

$T_b = K_t.I_b.f(\theta - 2\pi/3)$
(9)

$T_c = K_t.I_c.f(\theta - 2\pi/3)$
(10)

where, K_t is the torque constant

Total developed torque is given by:
$T_e = T_a + T_b + T_c$
(11)

C. Motion Equation:

The mechanical equations are
$J\,(d\omega_m/dt) + B\omega_m = T_e - T_l$
(12)

where, T_e = Developed electromagnetic torque, T_l = the load torque, ω_m = the angular velocity, p = the number of poles. The friction coefficient B is calculated from moment of inertia J and mechanical time constant, τ_m as follows:

$B = J/\tau_m$ and $d\theta/dt = (p/2).\omega_m$
(13)

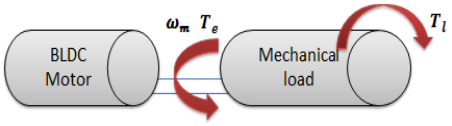

Fig. 6: Mechanical model of BLDC motor

Using KVL, the following equation is obtained,
$V_s = iR + Ldi/dt + e$
(14)

At steady state (DC state of zero-frequency), $V_s = iR + e$. Therefore, for the non-steady state, equation (14) is rearranged to make provision for the back emf, as shown below [9]:
$e = - iR - Ldi/dt + V_s$
(15)

where, V_s = the DC source voltage, i = the armature current

From the Newton's second law of motion, the mechanical properties relative to the torque of the system arrangement would be the product of the inertia load, J and the rate of angular velocity, ωm is equal to the sum of all the torques, these follow with equation (16) and (17) accordingly.

$J(d\omega_m)/dt = \sum T_i$
(16) $T_e = J(d\omega_m)/dt + T_l + B\omega_m$
(17)

The electrical torque and the back emf could be written as:
$e = k_e\omega_m$
(18) $Te = k_t i$
(19) where, k_e = the back emf constant; k_t = the torque constant.

Therefore, re-writing equations (15) and (16), the equation (20) and (21) are obtained as

$di/dt = - i(R/L) – (k_e/L)\omega_m + (1/L)V_s$

(20)

$d\omega_m/dt = i(k_t/J) – (B/J)\omega_m + (1/J)T_l$

(21)

Using Laplace transform in eq. (20) and eq. (21), the following equations are obtained considering all initial conditions are assumed to be zero.

$si = - i(R/L) – (k_e/L)\omega_m + (1/L)V_s$

(22)

$s\omega_m = i(k_t/J) – (B/J)\omega_m + (1/J)T_l$

(23)

At no load (for $T_l = 0$), $s\omega_m = i(k_t/J) – (B/J)\omega_m$

(24)

From eq. (24), i is found out as:

$$i = \frac{s\omega_m + \frac{k_f}{J}\omega_m}{\frac{k_t}{J}}$$

(25) By substituting eq. (25) in eq. (22), it becomes:

$$\left(\frac{s\omega_m + \frac{k_f}{J}\omega_m}{\frac{k_t}{J}}\right)\left(s + \frac{R}{L}\right) = \frac{-k_e}{L}\omega_m + \frac{1}{L}V_s$$

(26)

$$\left\{\left(\frac{s^2J}{k_t} + \frac{sk_f}{k_t} + \frac{sRJ}{k_tL} + \frac{k_fR}{k_tL}\right) + \frac{k_e}{L}\right\}\omega_m = \frac{1}{L}V_s$$

(27)

Therefore,

$$V_s = \left\{\frac{s^2JL+sLB+sRJ+BR+k_ek_t}{k_t}\right\}\omega_m$$

(28)

The transfer function is therefore obtained as follows using the ratio of the angular velocity, ω_m to source voltage, V_s.

$$G(s) = \frac{\omega_m}{V_s} = \frac{k_t}{s^2JL+s(RJ+LB)+RB+k_ek_t}$$

(29)

Considering the following assumptions:

1. The friction constant is small, that is, B tends to 0, and this implies that;
2. $RJ \gg BL$, and
3. $k_ek_t \gg RB$

The negligible values zeroed, the transfer function is finally written as

$$G(s) = \frac{\omega_m}{V_s} = \frac{k_t}{s^2JL+RJs+k_ek_t}$$

(30)

So by re-arrangement and mathematical manipulation on "JL", by multiplying top and bottom of equation (38) by: $\frac{R}{k_ek_t} \times \frac{1}{R}$

$$G(s) = \frac{\frac{1}{k_e}}{\frac{RL}{k_ek_tR}s^2 + \frac{RJ}{k_ek_t}s+1}$$

(31)

Substituting the mechanical time constant, $\tau_m = \frac{RJ}{k_ek_t}$ and the electrical (time constant), $\tau_e = \frac{L}{R}$ in eq. (32), we get

$$G(s) = \frac{\frac{1}{k_e}}{\tau_m\tau_es^2+\tau_ms+1}$$

(32)

D. Calculations:

BLDC motor with a symmetrical arrangement of Y-connected, three phase, the mechanical time constant and the electrical time constant becomes:

$$\tau_m = \sum\frac{RJ}{k_ek_t} = \frac{J3R}{k_ek_t}$$

(33)

$$\tau_e = \sum\frac{L}{R} = \frac{L}{3R}$$

(34)

Table-3 shows some of the important parameters used for motor modeling and calculations.

TABLE II. BLDC MOTOR PARAMETERS USED MODELING

Parameters	Value	Parameters	Value
Rs	1.20 Ω	**J**	9.25e-6
L	0.560e-3 H	τ_m	0.0171 s
Kt	25.5e-03	**Poles**	8
Ke	0.0763	**No. of phases**	3

By putting the motor parameter values in eq. (33) and eq. (34),

$$\tau_e = \frac{0.560 \times 10^{-3}}{3 \times 1.20} \quad \therefore \tau_e = 155.56 \times 10^{-6}$$

But τ_m is a function of R, J, K_e and K_t,

$$k_e = \frac{J3R}{\tau_m k_t} = \frac{3 \times 1.2 \times 9.25 \times 10^{-6}}{0.0171 \times 25.5 \times 10^{-3}} = 0.0763 \ \frac{v-s}{rad}$$

$$\therefore G(s) = \frac{13.11}{2.66 \times 10 - 6s^2 + 0.0171 \cdot s + 1}$$

The G(s) derived is the open loop transfer function of the BLDC motor using all necessarily sufficient parameters available.

V. BLOCK DIAGRAM OF BLDC MOTOR DRIVE WITH HYSTERESIS CURRENT CONTROLLER

The schematic block diagram of a BLDC motor drive with Hysteresis Current Controller is shown in Fig. 7. The drive consists of PID speed controller, Hysteresis Current Controller, reference current generator, position sensor decoder, the motor and the three phase inverter. In

conventional BLDC motor drive system, generally two control loops are used. The inner loop synchronizes the inverter gates signals with the back emf and the outer loop controls the speed of the motor. The actual speed of the motor is compared with the reference speed (ω_r) and the speed error is processed in PID controller. The output of the controller provides a constant voltage supply to the inverter. The inverter gates signals are produced by decoding the hall sensor signals of the motor. The three-phase voltage of the inverter is applied to the BLDC stator windings [10].

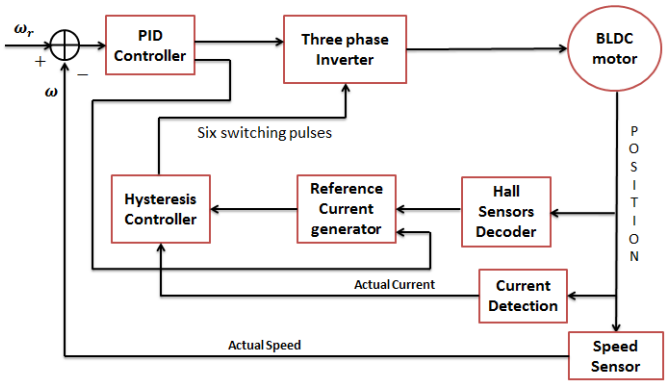

Fig. 7: Schematic block diagram of BLDC drive system with Hysteresis Current Controller

In this case, the actual stator winding currents of the motor are compared with the reference currents to generate and in turn switching pulses to drive the inverter switches. The reference current generator block generates three phase reference currents Ia_{ref}, Ib_{ref}, Ic_{ref} depending on the position of the rotor and in accordance with the value of PID speed controller and limiter. The reference current for each phase is function of the rotor position. In Table 3 the value of the reference current values with respect to the rotor positions are shown.

TABLE III. REFERENCE CURRENT W.R.T ROTOR POSITIONS

Rotor Position θ	Ia_{ref}	Ib_{ref}	Ic_{ref}
0 – π/3	I_s	$-I_s$	0
π/3 – 2π/3	I_s	0	$-I_s$
2π/3 – π	0	I_s	$-I_s$
π - 4π/3	$-I_s$	I_s	0
4π/3 - 5π/3	$-I_s$	0	I_s
5π/3 - 2π	0	$-I_s$	I_s

A. *Principle of Hysteresis Current Controller*

The Hysteresis Current Controller generates the switching gate pulses for the power semiconductor devices in the inverter. It works on pulse-width modulated (PWM) current control technique as shown in Fig. 7. It is an instantaneous current feedback control method in which the actual current continuously tracks the command current within a preassigned Hysteresis band. If the actual current exceeds the higher band, the upper switch of the half bridge becomes inactive and the lower switch becomes active. As the current decays and crosses the lower band, the lower switch becomes inactive and the upper switch becomes active. If Hysteresis band is reduced, then there is an improvement in the harmonic quality of the wave, but the switching frequency will increase, which in turn causes high switching losses [11].

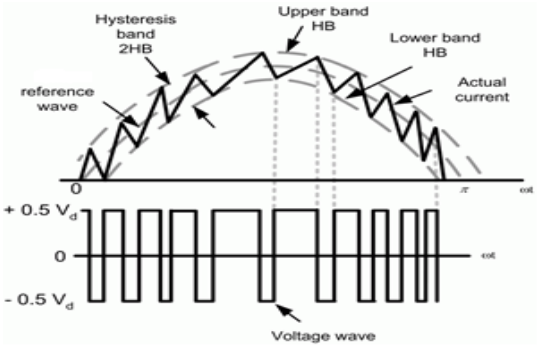

Fig. 8: Hysteresis Current Controller principle

VI. SIMULATION MODELS OF BLDC MOTOR DRIVES

The Simulink models of closed-loop BLDC motor drive system with and without Hysteresis Current Controller using MATLAB Simulink [12] are shown in Fig. 9 and Fig. 10 respectively.

A. *Conventional Closed-loop BLDC Motor Drive Simulink Model without Hysteresis Current Controller*

The Simulink model of conventional Brushless DC motor drive system model includes the following main modules: 1) BLDC motor module 2) PID controller module 3) Inverter module 4) Gate pulse switching module as shown in the Fig. 9.

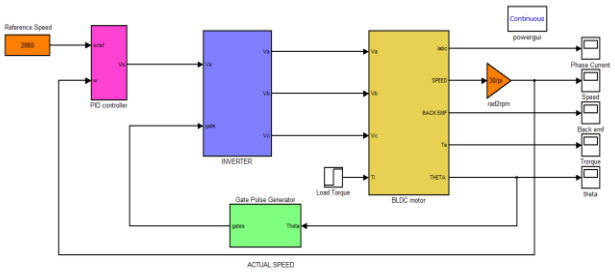

Fig. 9: Simulink model without Hysteresis Current Controller

B. *Closed-loop BLDC Motor Drive Simulink Model with Hysteresis Current Controller*

The Simulink model of conventional Brushless DC motor drive system model includes the following main modules: 1) BLDC motor module 2) PID controller 3) Inverter module 4) Reference current generator module 5) Hysteresis Current Controller module as shown in the Fig. 10.

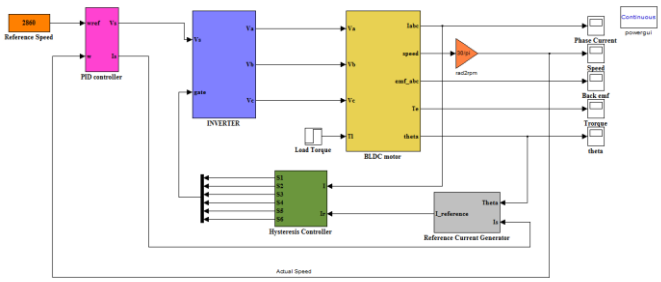

Fig. 10: Simulink model with Hysteresis Current Controller

The representation of modeling of the BLDC motor in accordance with the mathematical equations as derived in section 4 is inside the BLDC motor module. The output of the PID controller block is the sum of the proportional gain (k_p), integral gain (k_i), and derivative gain (k_d) which are the parameters of PID controller. The error signal generated by the difference between the reference speed and actual speed is the input signal of PID controller. The tuning of PID controller gains can be done either manually or automatically. For automatic tuning, Simulink® Control Design™ software (PID Tuner) is used [13].

VII. SIMULATION RESULTS

The closed-loop BLDC drives system with and without Hysteresis Current Controller were implemented & simulated successfully using MATLAB Simulink & the following results are generated. The simulation time is taken as 0.2 sec. The performance of the developed BLDCM drive system model is examined using Maxon EC 45 flat Ø45 mm, brushless, 30 Watt motor parameters [14]. At first, various waveforms related to BLDCM drive system without Hysteresis Current Controller is shown and then with Hysteresis Current Controller. For validation of work and results, comparison between the drives system are presented. The simulation is carried out for reference speed 2860 rpm and the load torque applied to the motor is set to step to its nominal value at time t = 0.1 sec. The simulation result shows for different parameters with respect to time.

A. Without Hysteresis Current Controller

The phase A stator winding current waveform are shown in Fig. 11. The three hall sensor signal outputs are decoded based on the evaluation of back emf waveform, as shown in Fig. 13. The gate pulse for the inverter switches are obtained by decoding the Hall Effect signals of the motor are shown in Fig. 12.

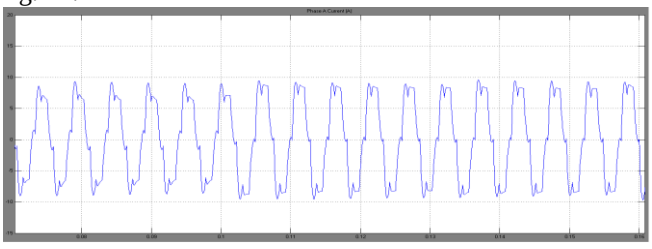

Fig.11: Phase A stator winding current of BLDC motor

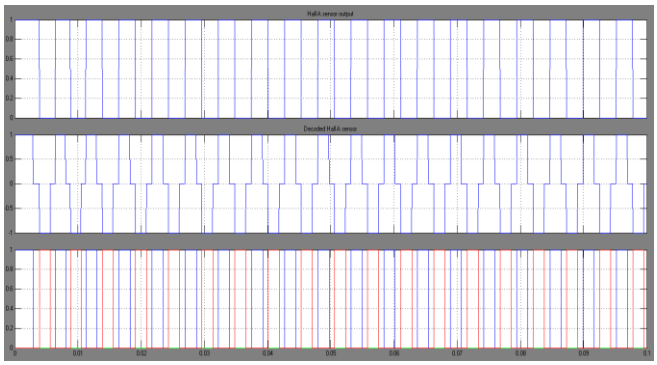

Fig-12: Hall sensor output, its decoded signal and gate pulses of inverter switches (Q1 & Q4) for leg A

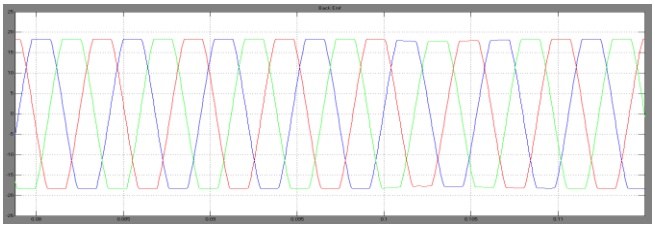

Fig. 13: Enlarged back emf voltage

The speed response of the motor at its nominal speed i,e 2860 rpm as shown in Fig. 14. The result reveals that the speed starts from zero rpm and rises upto 3300 rpm and attains speed at its steady value at t = 0.15 sec, but at t = 0.1 sec when the load torque is applied it falls down and again attains its speed at t = 0.11 sec.

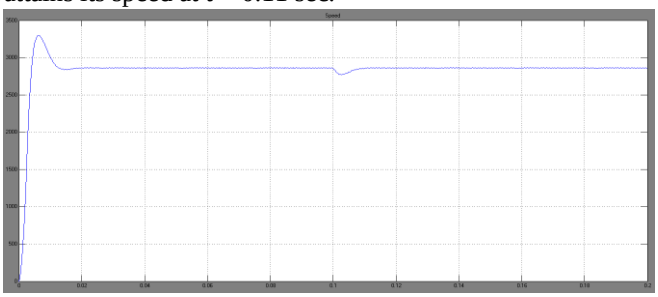

Fig. 14: Speed response at reference speed 2860 rpm

Fig. 15 shows the torque waveform. The motor is developing a torque of 1.15 Nm at the time of starting and develops a torque of 0.18 Nm at no load condition. At t=0.1s, motor is developing 0.23 Nm torque.

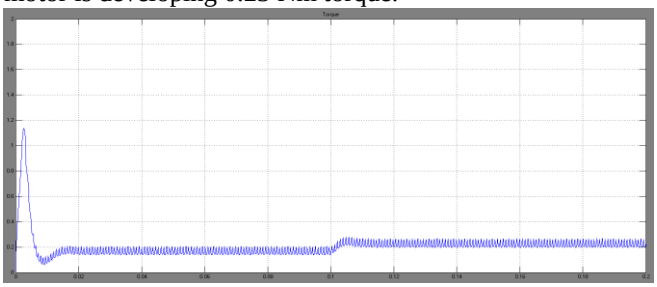

Fig. 15: Developed Torque waveform

B. With Hysteresis Current Controller

The waveforms for the actual stator current and reference current Ia_{ref} for phase A are shown in Fig. 16 and Fig. 17 respectively.

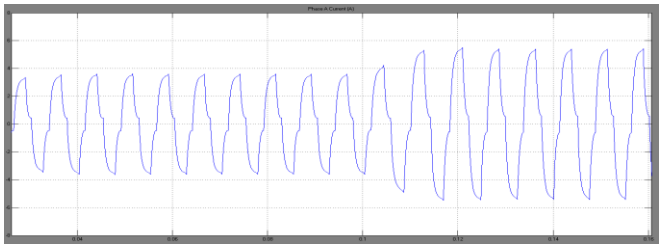

Fig. 16: Phase A actual stator current

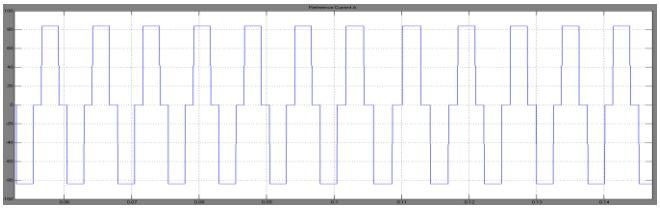

Fig. 17: Phase A reference current

The Fig. 18 shows the speed curve at nominal speed of the motor (i,e 2860 rpm). The result shows that the speed starts from zero rpm and rises upto 2950 rpm and attains the speed at steady state value at t=0.06 sec, but at t = 0.1 sec when the load torque is applied it falls down upto 2620 rpm and again attains its speed at t = 0.16 sec.

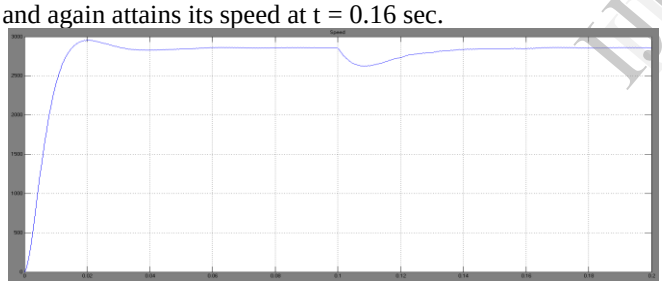

Fig. 18: Speed response at reference speed 2860 rpm

The Fig. 19 shows the developed torque waveform. The motor is developing a torque of 0.38 Nm at the time of starting and develops a torque of 0.16 Nm at no load condition. At t=0.1 sec, when load torque is applied 0.22 Nm torque is developed.

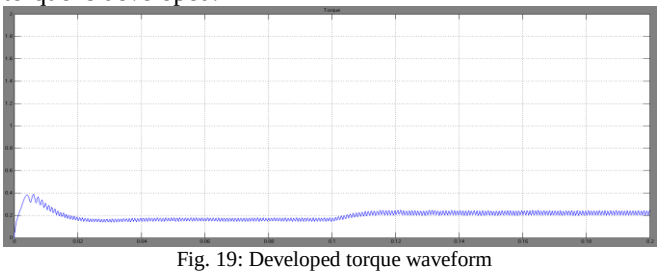

Fig. 19: Developed torque waveform

C. Comparison of BLDC drives with and without Hysteresis Current Controller

In this section, comparative waveforms of BLDCM drives with and without Hysteresis Current Controller are presented with the help of phase A stator winding currents and the developed torque of the motor as shown in Fig. 20 and Fig. 21 respectively.

A comparison table is also presented to show the magnitude of the peak current and torque and their ripple percentage are shown in Table IV. It is seen that the magnitude of peak current and torque are less with Hysteresis Current Controller as compared to without Hysteresis Current Controller.

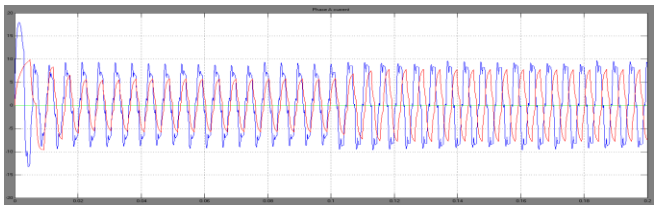

Fig. 20: Comparison waveform of phase A stator current with and without Hysteresis Current Controller

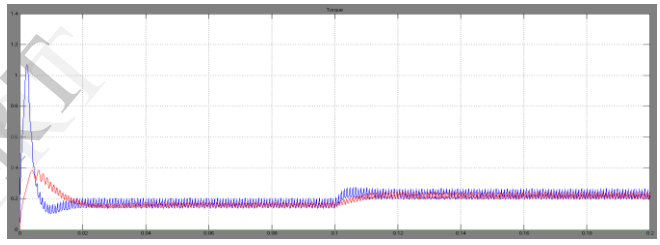

Fig. 21: Comparison waveform of torque with and without Hysteresis Current Controller

TABLE IV. COMPARISON TABLE

	Without Hysteresis	**With Hysteresis**
Phase current		
Magnitude of Peak Current	17.32 A	10A
Torque		
Magnitude of Peak Torque	1.14 Nm	0.38 Nm
Torque Ripple %	33.67%	20%

D. Speed Performance at different reference speed and at different load torque

At different speed with same load torque, motor dynamic behavior is analyzed as shown in Fig. 22. As the speed increases, rise time and the time required to reach the steady state speed also increases as shown in Table V.

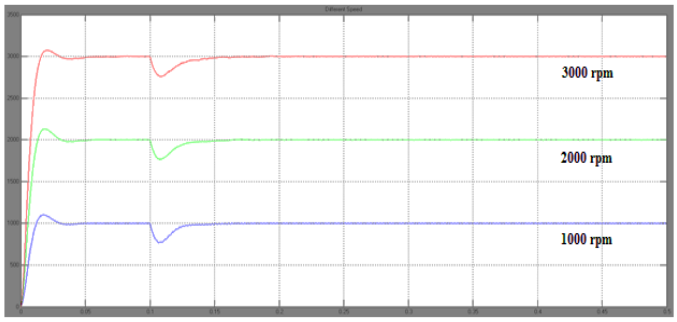

Fig. 22: Speed response at different speed

TABLE V. RISE TIME AND SETTLING TIME AT DIFFERENT SPEED

Set speed (rpm)	Rise time (s)	Settling time (s)
1000	0.065	0.145
2000	0.018	0.155
3000	0.02	0.16

The motor dynamic behavior is analyzed when different load torque is applied at time t = 0.1 s for the same speed (2000 rpm). When the load torque is applied, percentage of speed fall increases as the value of the load torque increases that can be clearly seen from Fig. 23.

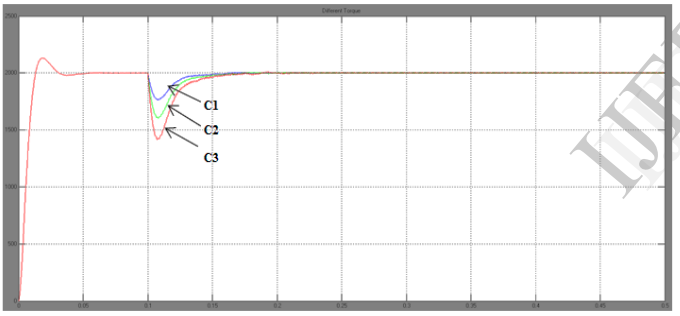

Fig. 23: Speed curve at different load torque

TABLE VI. SPEED CHARACTERISTICS AT DIFFERENT LOAD TORQUE

Curves	Load torque value	Set speed (rpm)	Speed fall %age
C1	0.059 Nm	2000	11.5
C2	0.1 Nm	2000	20
C3	0.15 Nm	2000	29

VIII. CONCLUSIONS

BLDC motor and its drive system modeling with different control schemes are implemented to control the speed, current and position in MATLAB Simulink and simulated results such as back emf, current speed response and developed torque response have been analyzed with and without Hysteresis Current Controller. The comparison of simulation result reveals that the Hysteresis Current Controller technique is more effective in reduction of torque ripples. This control method improves the system performance with low torque ripple thus making it suitable for immense applications.

ACKNOWLEDGMENT

I would like to thank everybody who has helped me in all possible ways towards successful completion of this work.

REFERENCES

[1] Huazhang WANG, "Design and Implementation of Brushless DC Motor Drive and Control System", Elsevier International Workshop on Information and Electronics Engineering (IWIEE), 2012.

[2] How to select Hall-effect sensors for brushless dc motors, Honeywell International Inc., 005959-1-EN, December 2012.

[3] Timothy L. Skvarenina. The Power Electronics Handbook. CRC Press, 2002, pp.10-11.

[4] Chang-liang Xia. Permanent Magnet Brushless DC Motor Drives and Controls. John Wiley & Sons, 2012, pp.5.

[5] M. B. B. Sharifian, M. Ebadpour, and S. A. KH. Mozaffari Niapour, "A New Cost Effective Single Current Strategy for Brushless DC Motor Drives", IEEE, 2012.

[6] P.Yedamale, Brushless DC (BLDC) Motor Fundamentals Application Note. AN885, Microchip; AZ, USA: 2003.

[7] Speed Control of Brushless DC Motors-Block Commutation with Hall Sensors, Microsemi User's Guide.

[8] R.Krishnan, "Permanent-Magnet Synchronous and Brushless DC Motor Drives", in Electric Motor Drives Modeling, Analysis and Control, Pearson Education Inc. Pearson Prentice Hall, © 2001, pp. 578-580.

[9] Bikram Das, Suvamit Chakraborty, Prabir Ranjan Kasari & Abanishwar Chakrabarti, "Reverse Regeneration Technique of BLDC Motor for Capacitor Charging", Proc. of the Intl. Conf. on Advances in Computing, Electronics and Communication (ACEC), 2013.

[10] Matlab R2010a Documentation on Brushless DC Motor Fed by Six-Step Inverter.

[11] Bimal Bose, "Voltage fed converters and PWM Techniques", Power Electronics and Motor Drives Advances and Trends, Elsevier, 2011, pp. 201-202.

[12] Simulation software-MATLAB 7.10.0 (R20010a).

[13] Matlab R2010a Help Documentation on PID Controller.

[14] Maxon EC 45 flat Ø45 mm, brushless, 30 Watt flat motor parameters datasheet.